Pergamon

*Int. J. Heat Mass Transfer.* Vol. 37, Suppl. 1, pp. 241–253, 1994

0017–9310/94 $6.00 + 0.00

0017–9310(93)E0055–L

# The effect of turbulent structures on the development of mixing and combustion processes in sub- and supersonic $H_2$ flames

M. HAIBEL and F. MAYINGER

Lehrstuhl A für Thermodynamik, Technische Universität München, Arcisstr. 21, D-80333 Munich, Germany

**Abstract**—The development and structure of the mixing and combustion process of sub- and supersonic hydrogen/air flames was investigated by means of optical measurement techniques. The experiments showed that the development of the mixing jet can be predicted with a new, given formula. The use of a rearward facing step enabled the stabilization of the flame under all operation conditions of the combustion chamber up to supersonic speed. A given model for the stabilization of high-speed hydrogen/air flames explains the influence of turbulent flow structures on the combustion process.

## 1. INTRODUCTION

COMBUSTION is still the most important way to provide thermal energy for application in power plants, heating and propulsion systems. Not only the efficiency but also the environmental impact of these systems are linked to the efficiency of the combustion process. The most common type of flames used in technical combustion systems are diffusion flames, where fuel and oxidizer enter the combustion chamber separately. They are mainly controlled by the mixing process of the utilized fuel and oxidizer (pure oxygen or air), as the time constant for mixing $\tau_{mix}$ is 5–6 orders of magnitude higher than the time constant for the chemical reaction $\tau_{chemical}$. This means that mixing is the leading control parameter for the efficiency of technical combustion processes. The mixing process itself is controlled by convective mass transfer and diffusion of the injected fuel and the surrounding air, and is influenced very much by turbulent structures in the flow field and the injector geometry.

In the past a huge number of theoretical and experimental works were published dealing with the injection and mixing of gaseous types of fuel into high speed air flows, focusing on high speed aircraft propulsion system applications [1–17]. The purpose of these papers was to describe the mixing process due to the penetration of the mixing jet into the surrounding air flow and the concentration profile of the mixing jet using different injector geometries. The goal of these investigations was to predict the behaviour of the upcoming flame for combustion chamber design. Figure 1 shows a sketch of a fuel/air mixing jet developing downstream of an injector geometry. The coordinate system is located in the centre of the injector nozzle with the $x$-axis in the direction of the initial air flow and the $y$-axis perpendicular to it. The former investigations showed that, in general, the spatial growth of the outer border of the mixing jet can be described by using a power law like

$$\frac{y}{d_0} = C \cdot \left(\frac{x}{d_0}\right)^{\beta} \tag{1}$$

where $\beta$ represents the growth rate of the mixing jet and the constant $C$ is a function of the used injector geometry and the initial fuel and air flow parameters.

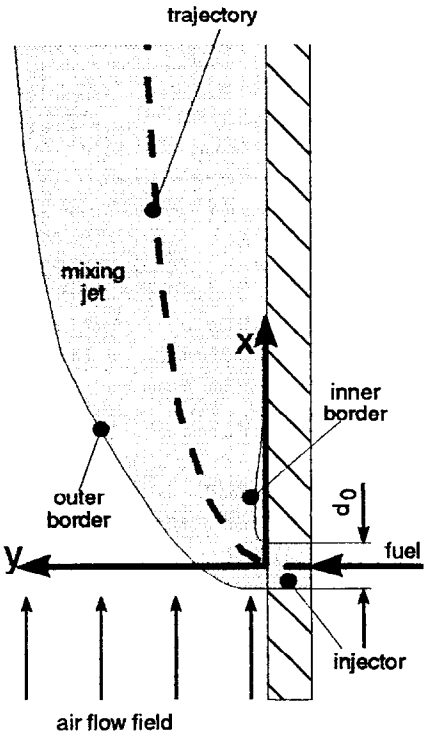


FIG. 1. Sketch of the mixing jet with cross flow in the vicinity of the fuel injection zone.

## NOMENCLATURE

| | |
|---|---|
| $C$ | constant in equation (1) |
| $d_0$ | diameter of the injector nozzle [mm] |
| $F/A$ | fuel/air mixing ratio |
| $I$ | specific momentum ratio of fuel and air, $(\rho w^2)_{\text{fuel}}/(\rho w^2)_{\text{air}}$ |
| $M_\infty$ | initial air Mach number |
| $M_{\text{He}}$ | Mach number of the helium jet at the exit cross-section of the injection nozzle |
| $p$ | pressure [Pa] |
| $p_{\text{air exit}}$ | static pressure of the air flow at the exit cross-section of the combustion chamber [Pa] |
| $p_{\text{ambient}}$ | static pressure of the ambient atmosphere at the exit cross-section of the combustion chamber [Pa] |
| $p_{0;\text{He}}$ | stagnation pressure of the helium at the exit cross-section of the injector nozzle [Pa] |
| $p_{\text{He}}$ | static pressure of the helium at the exit cross-section of the injector nozzle [Pa] |
| $R_{\text{He}}$ | specific gas constant of helium [J kg K$^{-1}$] |
| $T$ | temperature [K] |
| $T_{0;\text{He}}$ | stagnation temperature of the injected helium [K] |
| $T_0$ | initial air temperature in [K] |
| $Tu$ | degree of turbulence |
| $u_B$ | burning velocity in [m s$^{-1}$] |
| $u_F$ | local flow velocity in [m s$^{-1}$] |
| $x$ | coordinate in the direction of the initial air flow field |
| $y$ | coordinate normal to the direction of the initial air flow field. |

Greek symbols

| | |
|---|---|
| $\alpha$ | injection angle [°] |
| $\beta$ | growth exponent of the outer border of the mixing jet |
| $\gamma_{\text{He}}$ | exponent of the specific helium mass flow rate in equations (2) and (5) |
| $\gamma_M$ | exponent of the initial air Mach number in equations (2) and (5) |
| $\kappa$ | isentropic exponent |
| $(\rho w)_{\text{air}}$ | specific mass flow rate of air [kg m$^{-2}$s$^{-1}$] |
| $(\rho w)_{\text{He}}$ | specific mass flow rate of helium [kg m$^{-2}$s$^{-1}$] |
| $(\rho w)_{\text{He;crit.}}$ | critical specific mass flow rate of helium [kg m$^{-2}$s$^{-1}$] defined by equation (4) |
| $(\rho w)_{H_2}$ | specific mass flow rate of hydrogen [kg m$^{-2}$s$^{-1}$]. |

The object of this paper is to demonstrate the effect of turbulence on the development of the mixing jet and on the stabilization of hydrogen/air flames in the vicinity of a rearward facing step. Thereby the initial air flow velocity was varied within a wide range up to supersonic speed and a number of different types of injector geometries were investigated. The major difference to other experimental investigations is the use of non-preheated air and the use of a rearward facing step as a turbulence promotor. Wall effects of a duct flow concerning the growth of the mixing jet and the flame stabilization are also taken into account. The mixing and combustion processes were visualized using non-intrusive diagnostic methods such as holographic interferometry and OH self-fluorescence.

## 2. EXPERIMENTAL SETUP AND MEASUREMENT TECHNIQUE

The experimental investigations concerning the development and behaviour of the fuel/air mixing jets and of the combustion processes were performed in a combustion chamber sketched in Fig. 2. Pressurized air with a total temperature $T_0 = 291$ K was accelerated in an asymmetric, two-dimensional LAVAL nozzle with an exit cross-section of 30 mm × 15 mm. Thereby the air flow velocity could be varied between 25 m s$^{-1}$ ($M_\infty = 0.07$) and 445 m s$^{-1}$ ($M_\infty = 1.3$). The interchangeable injection block, which was linked to the gas supply system, was equipped with different injector geometries: single hole injectors with an injection angle of 90, 45 and 0°, respectively, and a twin hole injector and a slot injector with an injection angle of 45°. A rearward facing step downstream of the injection block was used to induce turbulent flow structures and to generate a turbulent recirculation zone for the enhancement of the mixing process and the stabilization of the flame. The step height of the rearward facing step could be varied between 0 and 10 mm. The side walls of the combustion chamber were equipped with quartz glass windows to receive transparency for optical measurement techniques in the visible and in the ultra-violet spectrum. The flame table downstream of the exit cross-section was, as well as the whole combustion chamber, not cooled and made of stainless steel.

The experiments were subdivided into two parts. The first part was the investigation of the mixing process in the near field of the injector. These experiments were done without combustion ('cold mixing') using helium as a substitute for hydrogen. The second part dealt with the investigation of the combustion process concerning the stabilization and the behaviour of the hydrogen/air flames.

The mixing processes of helium and air were investigated by means of holographic interferometry using

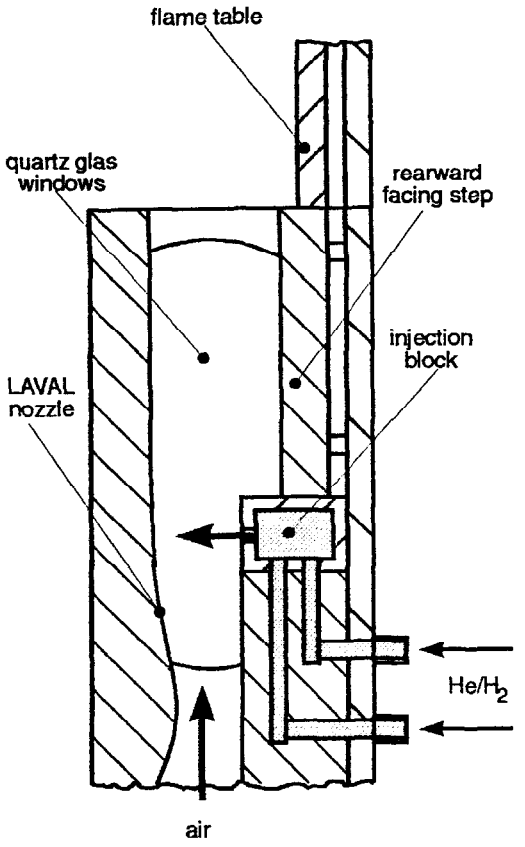


FIG. 2. Sketch of the combustion chamber.

the 'finite fringe' method. Thereby the deformation of a pattern of initially parallel fringes due to the injection of helium into the air flow was a direct measure for the concentration distribution inside the mixing jet. This deformation could be observed in real time on a projection screen and was monitored using an intensified CCD camera with very short exposure time of only 100 ns, so even highly dynamic processes could be recorded. The interferograms were analysed with respect to the spatial growth, the penetration, the concentration profile and the temporal fluctuation of the mixing jet. More detailed information on the holographic interferometry technique is given in refs. [18–21].

The combustion processes concerning the stabilization, the length and the structure of the high-speed hydrogen/air flames were investigated by means of OH self-fluorescence [19, 20, 22]. In the course of the $H_2/O_2$ reaction, the 21 single reaction steps can be subdivided into two blocks of chemical reactions, endothermal and exothermal. The transition from the endothermal into the exothermal block is characterized by the appearance of the OH radical. This means that the OH radical indicates the actual reaction front of the flame. In the course of this transition, the OH radicals emit light in the near ultra-violet spectrum within a wavelength band of 280–350 nm, with a strong band head at 306.7 nm. This phenomenon of light emission is called chemoluminiscence or self-fluorescence [22–24]. The spatial and temporal distribution of the reaction front in high-speed hydrogen/air flames were determined by recording the OH self-fluorescence using a UV-intensified CCD camera equipped with a small-banded interference filter with a centre wavelength of 308 nm.

## 3. RESULTS AND DISCUSSION

### 3.1. *Development and behaviour of the helium/air mixing jet*

The investigation of the development and behaviour of the helium/air mixing jet was conducted without combustion by means of holographic interferometry (see Section 1). Figure 3 shows a series of interferograms demonstrating the dependency of the helium/air mixing jet on the initial air Mach number $M_\infty$, which was determined immediately in front of the injector. The injection of the helium was realized with a single hole injector perpendicular to the air flow direction ($\alpha = 90°$). The helium mass flow rate was 1.46 g s$^{-1}$ (specific mass flow rate: $(\rho w)_{He} = 116.2$ kg m$^{-2}$ s$^{-1}$) and constant for all air Mach numbers. The height of the rearward facing step was 10 mm, which is 25% of the total combustion chamber height. The air flow velocity varied between 27 m s$^{-1}$ ($M_\infty = 0.08$) and 354 m s$^{-1}$ ($M_\infty = 1.17$).

It can be seen that with an initial air Mach number of $M_\infty = 0.08$, the parallel fringe pattern of the interferogram downstream of the injector is undeformed. This means that the whole combustion chamber is filled with a homogeneous mixture of helium and air. When increasing the air Mach number to $M_\infty = 0.25$, the mixing jet penetrates deep into the air flow and is quickly deflected towards the air flow direction. It can be seen, that the outer border of the mixing jet is very ragged, which indicates the impact of macroscopic and microscopic vortices on this free mixing shear layer. A further increase of the air Mach number leads to a decrease of the penetration and to a stronger deflection of the mixing jet, as the specific momentum ratio of helium and air, $I = (\rho w)_{He}/(\rho w)_{air}$, decreases. This means, that the mixing jet becomes more and more slender, though the outer border stays very ragged.

When reaching supersonic air velocity ($M_\infty = 1.11$), the mixing jet becomes very slender and unites with the free shear layer in the wake of the rearward-facing step. This presented case of supersonic flow is an adapted nozzle flow, which implies that the static pressure of the air flow at the exit cross-section of the combustion chamber is identical with the static pressure of the ambient atmosphere ($p_{air;exit} = p_{ambient}$). The last interferogram of this series shows the mixing jet in an underexpanded nozzle flow ($p_{air;exit} > p_{ambient}$). In this case, the mixing jet is very thin and collapses with the free shear layer in the wake

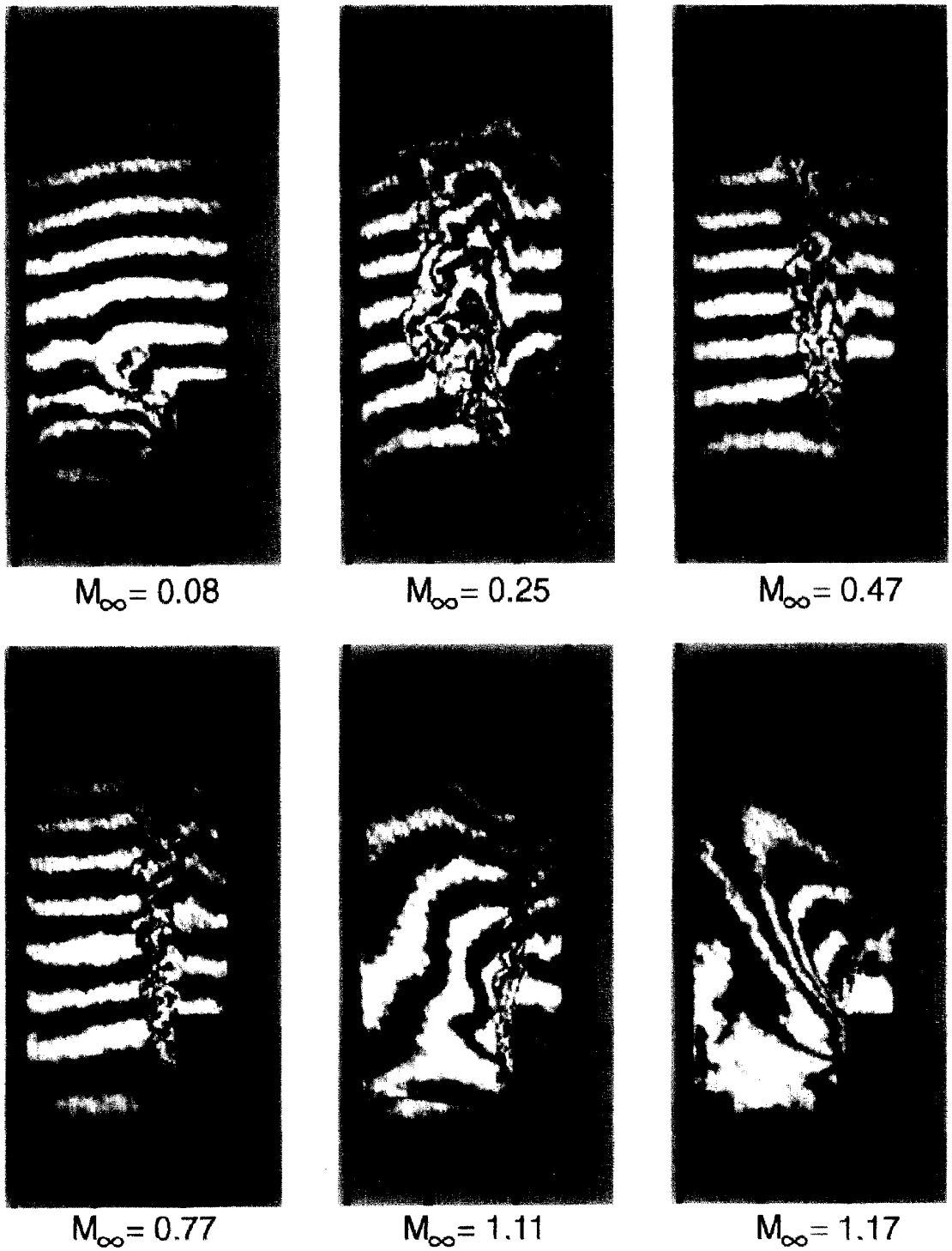


FIG. 3. Influence of the initial air Mach number $M_\infty$ on the development of the mixing jet recorded by means of holographic interferometry (single hole injector, $\alpha = 90°$, $(\rho w)_{He} = 116.2$ kg m$^{-2}$ s$^{-1}$).

of the rearward facing step, which is pushed towards the bottom of the step due to a pressure gradient between the main air flow and the recirculation zone. In addition to that, the interferogram shows an expansion/recompression shock wave system, which is generated due to the deflection of the main air flow field in the vicinity of the rearward facing step.

Figure 3 shows in general the strong dependency of the penetration and the structure of the mixing jet on the initial air Mach number $M_\infty$.

Figure 4 shows a series of interferograms indicating the dependency of the mixing jet structure on the injection angle $\alpha$ using a single hole injector. The initial air Mach number was set to $M_\infty = 0.8$ and the

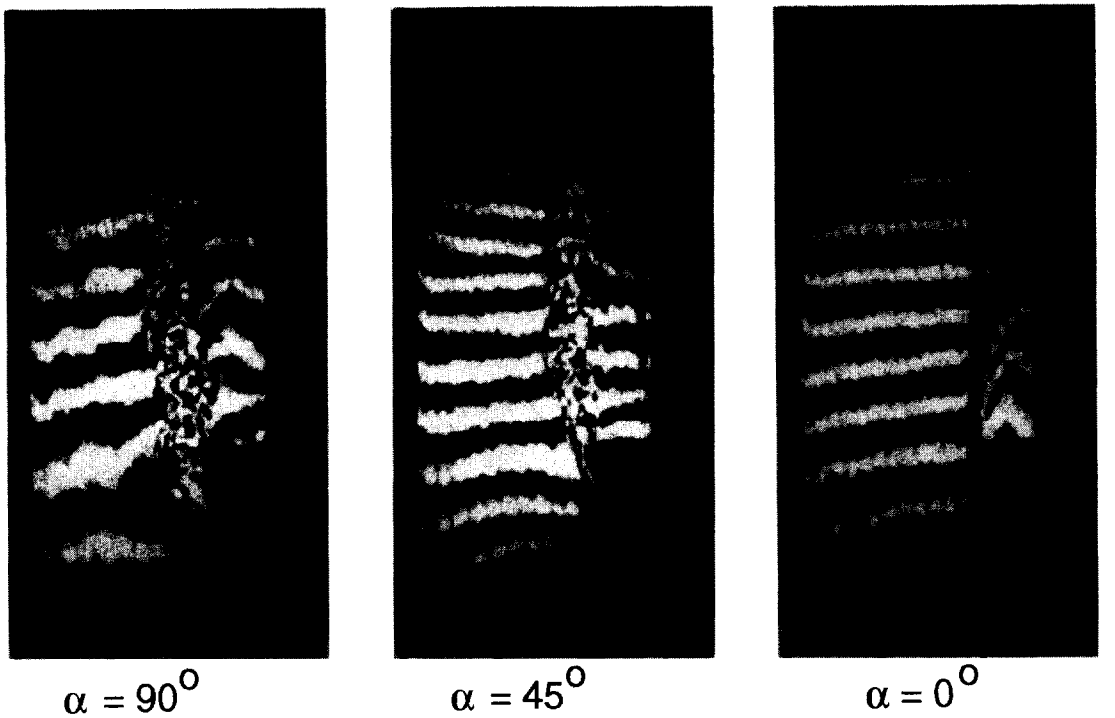


FIG. 4. Influence of the injection angle $\alpha$ on the development of the mixing jet recorded by means of holographic interferometry (single hole injector, $M_\infty = 0.8$, $(\rho w)_{He} = 206.9$ kg m$^{-2}$ s$^{-1}$).

injected helium mass flow rate was 2.6 g s$^{-1}$ ($(\rho w)_{He} = 206.9$ kg m$^{-2}$ s$^{-1}$). It can be seen that the growth rate and the penetration of the mixing jet decreases with decreasing injection angle from $\alpha = 90$ to 45°. On the other hand, the surface of the outer border is smoothed and the disturbance of the main flow field decreases with decreasing injection angle. Using a parallel injector ($\alpha = 0°$), the mixing jet does not penetrate into the main air flow field and the outer border of the jet is identical with the free shear layer, generated in the wake of the rearward facing step. Approximately 30 mm downstream of the injection zone, the mixing jet is broken up by the impact of vortices, and from there on the mixing process is enhanced by means of induced turbulent flow structures.

This series of interferograms shows that the structure and development of the mixing jet with respect to the penetration and growth rate is very much dependent on the injection angle $\alpha$ used.

Figure 5 indicates the dependency of the employed geometry on the mixing jet development. The figure shows the comparison of the mixing jet when using a single hole injector, a twin hole injector and a slot injector, respectively. The initial air Mach number was set to $M_\infty = 0.8$. The helium was injected with an injection angle of $\alpha = 45°$ with a mass flow rate of 1.46 g s$^{-1}$ ($(\rho w)_{He} = 116.2$ kg m$^{-2}$ s$^{-1}$).

It can be seen that the single hole injector causes a higher penetration and a greater thickness of the mixing jet compared with the twin hole injector. The slot injector effects the lowest penetration and the smallest thickness. When using a single hole injector, the mixing jet is not in contact with the side walls of the combustion chamber. This causes a three-dimensional turbulent air flow structure around the mixing jet, generating a pair of large-scale vortices in the wake of the jet. These vortices deform the initially circular cross-section of the mixing jet into a kidney-shaped cross-section, and thereby enhances the mixing rate due to an increase of turbulence-induced convective mass transfer [15]. When using a twin hole injector, this three-dimensional flow structure around the mixing jet is generated only within the first 10–15 mm downstream of the injection zone. Afterwards, the two single jets unite in the middle of the flow field and are in contact with the combustion chamber side walls, respectively. This means that downstream of this point, the mixing jet acts as a dividing layer between the main air flow and the flow field in the wake of the rearward facing step, and that there is no further flow structure around the jet to enhance the mixing process. This leads to a strong decrease in the mixing rate and the penetration depth.

When using a slot injector, the mixing jet is in contact with the side walls of the combustion chamber from the beginning of the mixing process, causing a permanent dividing layer between the main air flow and the flow field in the wake of the rearward facing step. This leads to a very poor mixing rate and small penetration of the mixing jet. These results concerning the influence of the injector geometry used on the development and behaviour of the mixing jet are also indicated when looking at the possibility of flame stabilization described in Section 3.2 below: the poorer the mixing rate in the jet and the poorer the

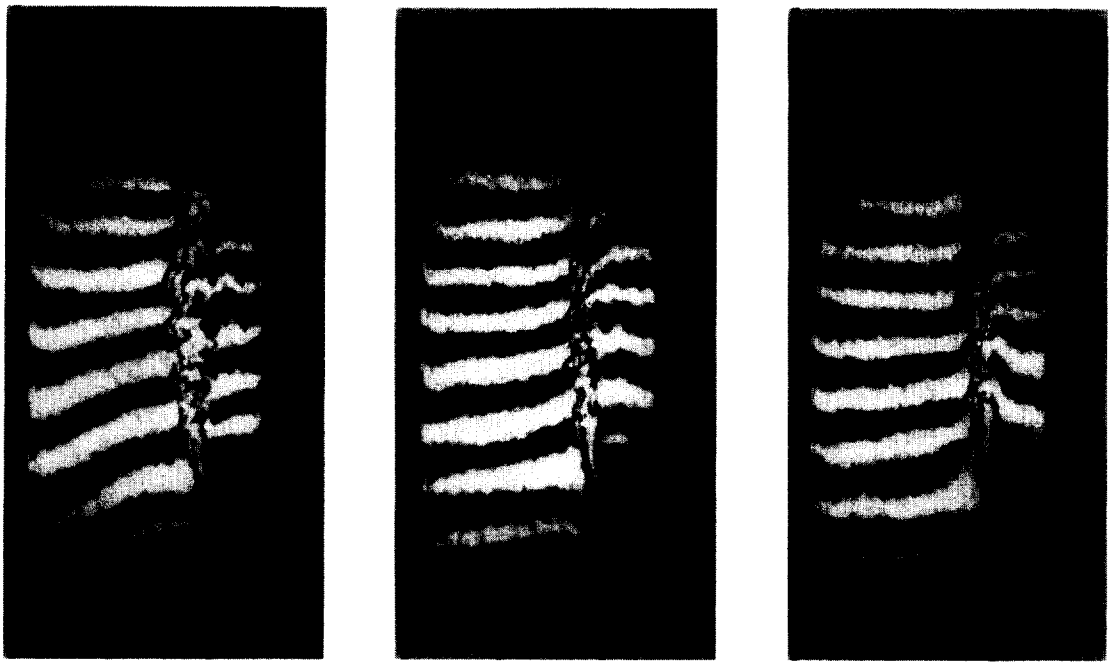


FIG. 5. Influence of the injector geometry (single hole, twin hole, slot) on the development of the mixing jet recorded by means of holographic interferometry ($M_\infty = 0.8$, $\alpha = 45°$, $(\rho w)_{He} = 116.2$ kg m$^{-2}$ s$^{-1}$).

three-dimensional flow structure around the jet inducing turbulence to the combustible mixture, the poorer the possibility to stabilize the flame.

As already mentioned in Section 1, the growth of the outer border of the mixing can be described by a power law (equation (1)). In this equation the coordinates $x$ and $y$ are normalized with the injector diameter $d_0$. When modifying this equation, the development of the outer border of the mixing jet for the perpendicular injection of helium into the air flow field ($\alpha = 90°$) can be described by the upcoming equation (2)

$$\frac{y}{d_0} = 1.5961 \cdot \left(\frac{(\rho w)_{He}}{(\rho w)_{He;crit.}}\right)^{0.65} \cdot M_\infty^{-1.15} \cdot \left(\frac{x}{d_0} + 0.01\right)^{0.0866} \quad (2)$$

with $M_\infty$ as the initial air Mach number and $(\rho w)_{He}$ as the specific mass flow rate of the injected helium (in kg m$^{-2}$ s$^{-1}$). $(\rho w)_{He;crit.}$ is the critical specific mass flow rate of the injected helium, defined as the maximum specific mass flow rate (in kg m$^{-2}$ s$^{-1}$) which arises when the Mach number of the helium jet at the exit cross-section of the injection nozzle appears to be equal to unity for the first time ($M_{He} = 1$). The critical specific mass flow rate $(\rho w)_{He;crit.}$ can be calculated as follows. Knowing the static pressure $p_{He}$ at the exit cross-section of the injection nozzle, the minimum stagnation pressure $P_{0;He}$ for the critical flow conditions of the helium can be calculated by

$$\left(\frac{p_{He}}{p_{0;He}}\right)_{crit} = \left(\frac{2}{\kappa+1}\right)^{\kappa/(\kappa-1)}. \quad (3)$$

Hence the isentropic exponent for helium is given by $\kappa = 1.63$. The static pressure for the described experiments was $p_{He} = 0.9703 \times 10^5$ (Pa), so the stagnation pressure was calculated to be $p_{0,He} = 1.9706 \times 10^5$ (Pa). Using the well-known formula for the determination of the critical specific mass flow rate

$$(\rho w)_{He;crit.} = \left(\frac{2}{\kappa+1}\right)^{1/(\kappa-1)} \cdot \sqrt{\left(\frac{\kappa}{\kappa+1}\right)} \cdot p_{0,He} \cdot \sqrt{\left(\frac{2}{R_{He} \cdot T_{0;He}}\right)} \quad (4)$$

the critical specific mass flow rate of helium for the described experiments was calculated to be $(\rho w)_{He;crit.} = 182.68$ (kg m$^{-2}$ s$^{-1}$). $R_{He}$ was the specific gas constant of helium and $T_{0;He} = 291$ (K) was the stagnation temperature of the injected helium.

Equation (2) shows that the growth exponent for the outer border of the mixing jet $\beta = 0.0866$ is identical with the one determined by Orth and Funk [23] for the normal injection of hydrogen into a high-speed air flow. The exponent of the specific mass flow rate of helium $\gamma_{He} = 0.65$ indicates the tendency of the mixing jet of penetrating deeper into the surrounding

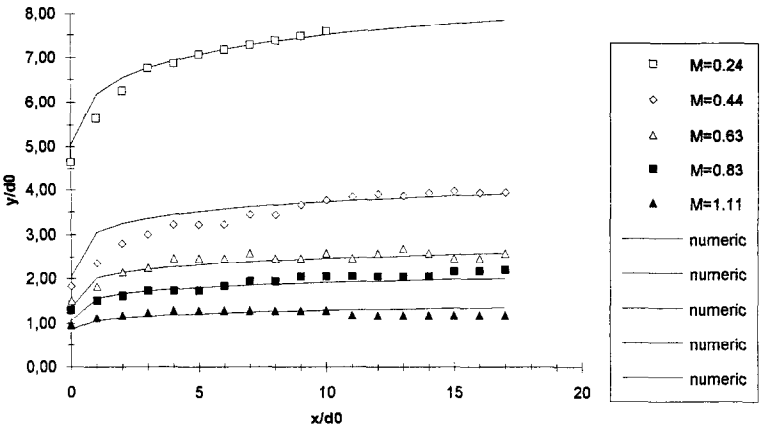


FIG. 6. Development of the outer border of the mixing jet at differential initial air Mach numbers $M_\infty$: comparison of experimental data with numerical simulation using equation (2) ($\alpha = 90°$, $(\rho w)_{He} = 116.2$ kg m$^{-2}$ s$^{-1}$).

air flow field with increasing helium mass flow rate. The exponent of the initial air Mach number $\gamma_M = -1.15$ expresses the fact that the mixing jet was more and more compressed and the penetration depth decreases with an increasing air Mach number.

In Fig. 6 the development of the outer border of the mixing jet with perpendicular helium injection is depicted. The figure shows the comparison of the received experimental data and the calculation using equation (2). It can be seen that the correspondence between experimental data and the calculation is very good over the whole range of the initial air Mach numbers. Equation (2) presumes adapted nozzle flow conditions for the air flow field, so the calculations did not fit with the under-expanded flow field shown in the last picture of Fig. 3.

The evaluations of the experimental data for the single hole injection of helium using an injection angle of $\alpha = 45°$ led to a similar equation but different exponents of the specific helium mass flow, the initial air Mach number and the growth rate of the mixing jet.

$$\frac{y}{d_0} = 1.034 \cdot \left(\frac{(\rho w)_{He}}{(\rho w)_{He;crit.}}\right)^{0.25} \cdot M_\infty^{-0.78} \cdot \left(\frac{x}{d_0} + 0.01\right)^{0.2}. \quad (5)$$

The growth exponent $\beta = 0.2$ is greater than the exponent for the perpendicular injection case. This indicates that using an injection angle of $\alpha = 45°$, the slope of the outer border of the mixing jet is flatter and that, compared with a 90° injector, the deflection of the jet due to the impact of the main air flow field occurs later downstream of the injection zone. Nevertheless it has to be taken into account that the smaller exponent for the specific mass flow rate of helium $\gamma_{He} = 0.25$ and the greater exponent of the initial air Mach number $\gamma_M = -0.78$ affects a smaller overall penetration of the mixing jet compared with the perpendicular injection. Furthermore the numerical values of these exponents indicate that the influence of the specific mass flow rate of helium and of the initial air Mach number on the development of the mixing jet is smaller when using an injection angle of $\alpha = 45°$ compared with an injection angle of 90°.

### 3.2. *Structure of the sub- and supersonic* $H_2$*/air flames*

Figure 7 shows the image of the reaction front distribution of a high-speed hydrogen/air flame recorded by means of OH self-fluorescence (see Section 1). The initial air Mach number was $M_\infty = 0.93$. Hydrogen was injected with a single hole injector using an injection angle of $\alpha = 45°$ with a specific mass flow rate of $(\rho w)_{H_2} = 159.2$ kg m$^{-2}$ s$^{-1}$. It can be seen that the flame was stabilized in the wake of the rearward facing step. Detailed investigations showed that the stabilization zone was located inside the turbulent free shear layer, separating the mixing jet and the recirculation zone in the wake of the rearward facing step. The highest reaction rate of the hydrogen/air flame could be observed downstream of the exit cross-section of the combustion chamber. Outside of the combustion chamber, the penetration of the flame into the air flow field increased as the influence of the combustion chamber walls disappeared.

The OH self-fluorescence method is a measurement technique which integrates over the whole depth of the optical path, leading to a two-dimensional image of the flame. To investigate the three-dimensional structure of the flames it is necessary to have at least two images of the flame recorded simultaneously under different directions [22]. Figure 8 shows the top view and the side view of the reaction front distribution of two hydrogen/air flames recorded simultaneously under two perpendicular directions downstream of the exit cross-section of the combustion chamber. The hydrogen was injected with an injection angle of $\alpha = 45°$ using a single hole injector. The specific mass flow rate of the hydrogen was

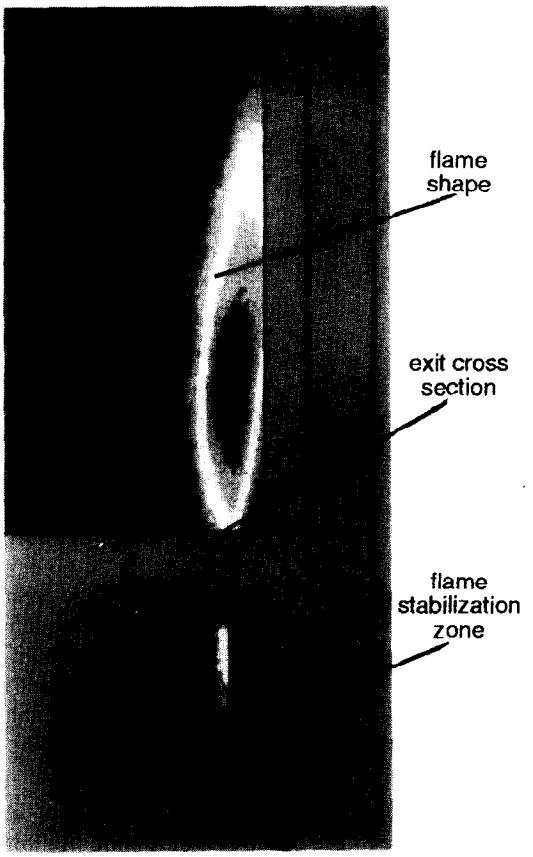


FIG. 7. Image of the reaction front distribution of a high-speed hydrogen/air flame recorded by means of OH self-fluorescence ($M_{\infty} = 0.93$, single hole injector, $\alpha = 45°$, $(\rho w)_{H_2} = 159.2$ kg m$^{-2}$ s$^{-1}$).

$(\rho w)_{H_2} = 109.0$ kg m$^{-2}$ s$^{-1}$, the initial air Mach numbers were $M_{\infty} = 0.6$ (A) and $M_{\infty} = 0.81$ (B).

When looking at the flame with $M_{\infty} = 0.6$, it can be seen that the region of high combustion intensity in the centre of the flame as indicated in the side view is not a closed area but a pair of stable vortices generated in the wake of the exit cross-section as depicted in the top view. When increasing the initial air Mach number to $M_{\infty} = 0.81$, this pair of vortices unite in the centre of the flame. Furthermore, it can be seen that there is a flame lift-off with increasing air Mach number due to an insufficient mixing rate, and thereby an insufficient supply of oxygen in the mixing jet inside the combustion chamber. This corresponds to the results of the cold mixing experiments presented in the previous section of this article. Another interesting observation is the decrease of the flame length with increasing initial air Mach number and the appearance of a wavy structure on the surface of the flame shape. The nature of this wavy structure is up to now not fully understood, but it is supposed, that it is caused by resonant flame oscillations influenced by the acoustic waves generated inside the combustion chamber.

The experiments have shown that the development and the behaviour of the high-speed hydrogen/air flames were, in general, very much influenced by the turbulent flow structure of the mixing jet and of the main air flow. Increasing turbulence led to an increase of the overall reaction rate and to a stirring-up of the combustion process.

### 3.3. *Conditions and parameters for the stabilization of high-speed* $H_2$*/air flame*

Figure 9 shows the comparison of a helium/air mixing jet and a hydrogen/air flame, both recorded in the vicinity of the rearward facing step inside the combustion chamber. The adjusted flow conditions were identical, with an initial air Mach number $M_{\infty} = 0.8$ and an injected mass flow rate of $(\rho w)_{He/H_2} = 79.2$ kg m$^{-2}$ s$^{-1}$ using a single hole injector ($\alpha = 45°$). When comparing these two images, it can be seen that combustion appears for the first time inside the free shear layer which separates the mixing jet and the recirculation zone in the wake of the rearward facing step. Downstream of that flame stabilization zone, where the flame is suspended, the reaction zone spreads towards the wake flow, where the interferogram predicts a combustible hydrogen/air mixture. Another interesting observation is that the flame does not move beyond the trajectory of the mixing jet into the main air flow. Therefore, the trajectory is defined as the line of the maximum local hydrogen concentration inside of the mixing jet [15].

The experimental investigations of the sub- and supersonic hydrogen/air flames, executed with a huge variety of injection geometries, injection angles, heights of the rearward facing step and specific mass flow rates for hydrogen in a wide range of initial air Mach numbers, led to a model for predicting the possibility of stabilization of high-speed hydrogen/air flames in the wake of rearward facing steps. Flame stabilization means that the burning velocity $u_B$ is identical with the local flow velocity $u_F$

$$u_B = -u_F. \tag{6}$$

The burning velocity $u_B$ is characterized as a function of the fuel/air mixing ratio $F/A$ with its maximum in the vicinity of stoichiometry and thermodynamic properties such as pressure $p$ and temperature $T$, and is mainly controlled by the degree of turbulence $Tu$ in the combustible mixture [25, 26]

$$u_B = f(F/A; p; T; Tu). \tag{7}$$

Experiments have shown that turbulence is able to increase the burning velocity up to numbers 100-times higher than the laminar burning velocity.

Figure 10 shows a sketch of the flow field in the vicinity of the fuel injector and the rearward facing step. The mixing jet and the recirculation zone in the wake of the rearward-facing step is separated by a turbulent free shear layer, which is characterized by the inner border of the mixing jet. Inside the free shear layer, the greatest gradients of the flow velocity and thereby the highest degrees of turbulence of the whole combustion chamber flow field occur. On the other hand, the inner border of the mixing jet is char-

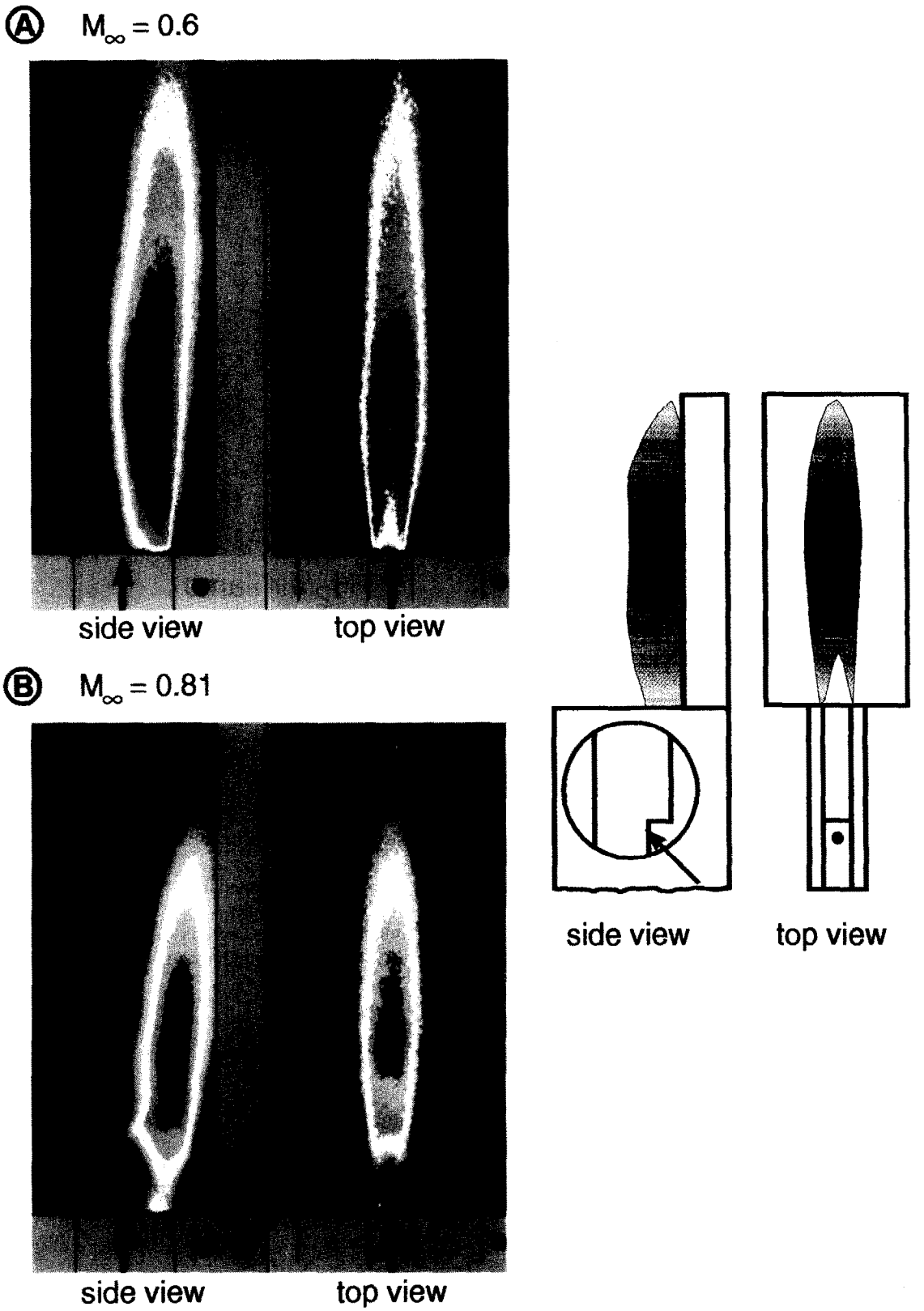


FIG. 8. Top view and side view of the reaction front distribution of a hydrogen/air flame with an initial air Mach number of (A) $M_\infty = 0.6$ and (B) $M_\infty = 0.81$; the images were taken downstream of the exit cross-section of the combustion chamber, as illustrated in the right sketch (single hole injector, $\alpha = 45°$, $(\rho w)_{H_2} = 109.0\ \mathrm{kg\ m^{-2}\ s^{-1}}$).

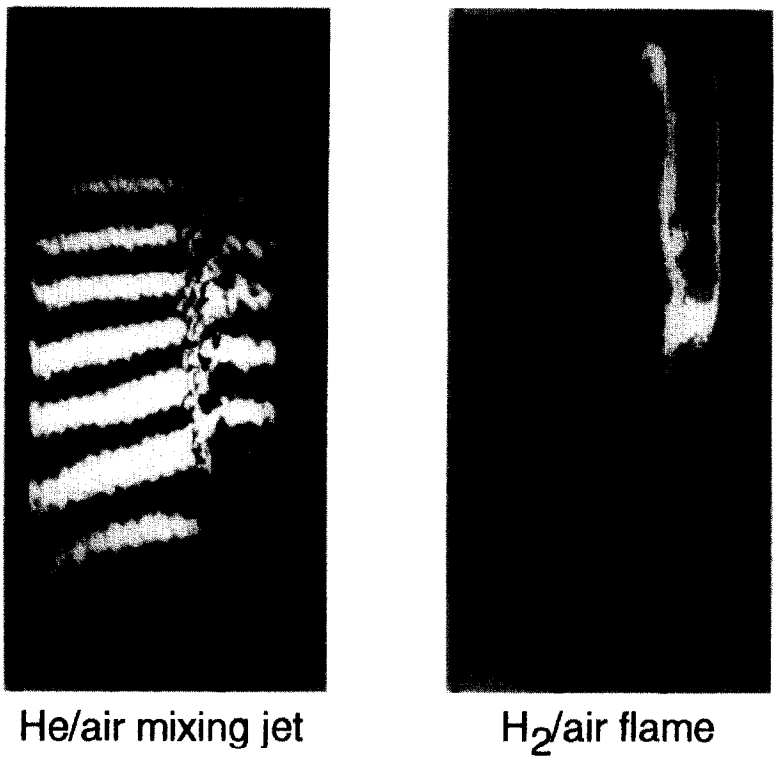


FIG. 9. Comparison of the helium/air mixing jet with the hydrogen/air flame in the vicinity of the rearward facing step inside the combustion chamber ($M_\infty = 0.8$, single hole injector, $\alpha = 45°$, $(\rho w)_{He,H_2} = 79.2$ kg m$^{-2}$ s$^{-1}$).

acterized by a near-stoichiometric fuel/air mixture. This means that this free shear layer provides the best conditions for flame stabilization in the entire combustion chamber, as the flow velocities are relatively low and the burning velocities are high due to the high degree of turbulence. Therefore, the flame is predicted to be stabilized at the inner border of the mixing jet. All performed experiments proved this.

Another region in the vicinity of the mixing jet where these conditions for flame stabilization—apart from the low flow velocity—occur, is the outer border of the mixing jet. It could be observed that using low initial air Mach number of up to $M_\infty = 0.1$, the flame was stabilized also within the outer free shear layer of the mixing jet. But when increasing the initial air Mach number, the flame was blown off at the outer border as the local flow velocity became greater than the burning velocity.

All up-to-now presented images of sub- and supersonic hydrogen/air flames were recorded by means of OH self-fluorescence using an exposure time of 1 ms for each image. When reducing the exposure time to

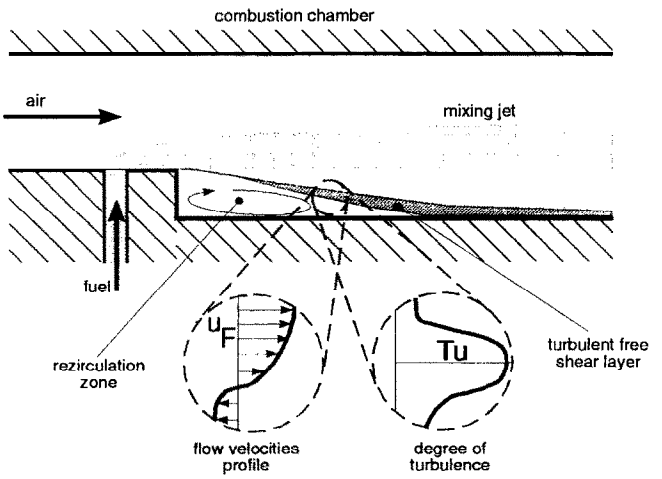


FIG. 10. Sketch of the flow field in the vicinity of the injection zone and rearward facing step.

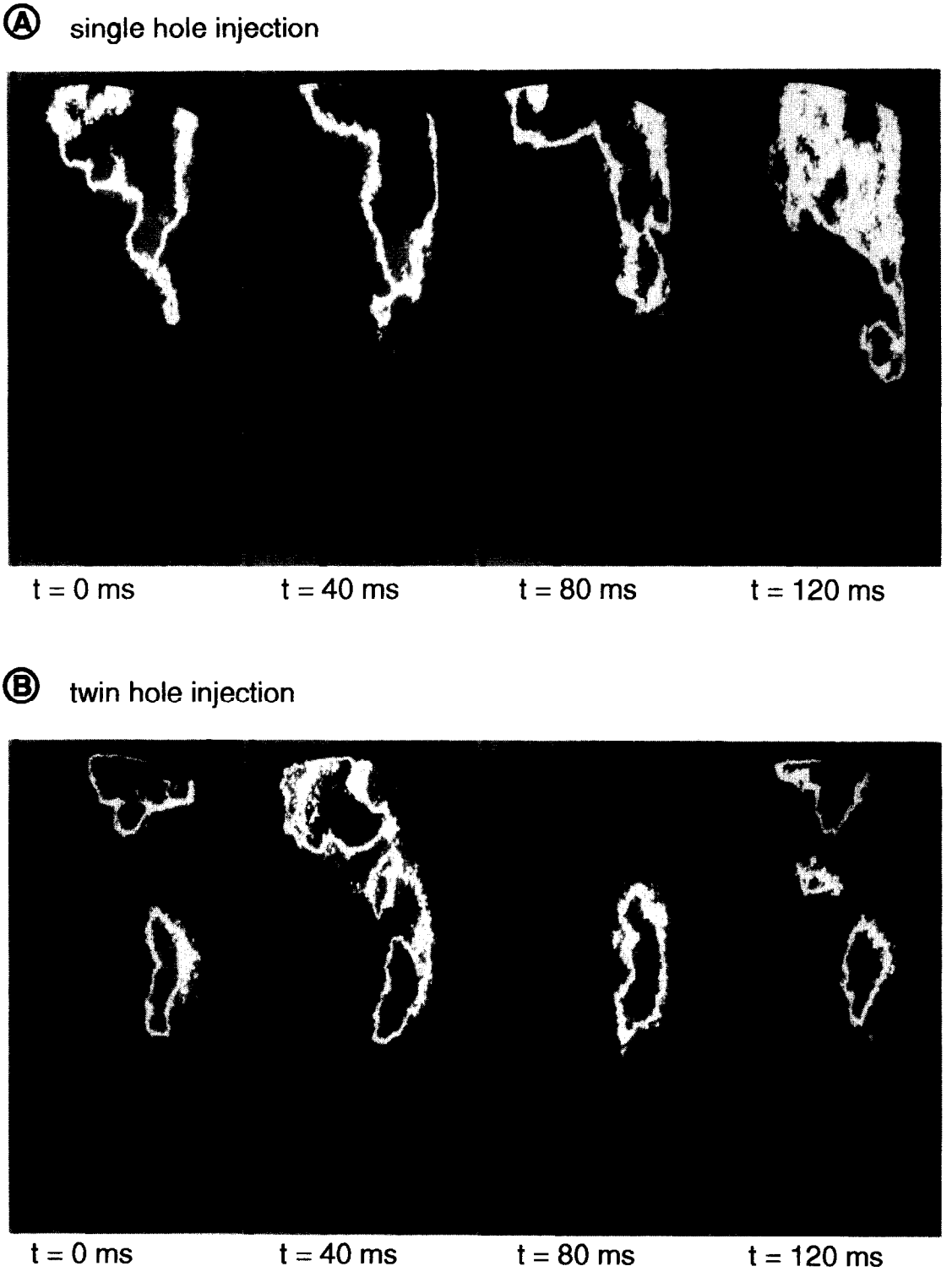


FIG. 11. Temporal behaviour of the flame oscillations in the vicinity of the rearward facing step inside the combustion chamber recorded in time steps of 40 ms using an exposure time of 5 $\mu$s; (A) single hole injector, (B) twin hole injector ($M_\infty = 0.2$, $\alpha = 45°$, $(\rho w)_{H_2} = 55.7$ kg m$^{-2}$ s$^{-1}$).

only 5 $\mu$s, stable fluctuations of the reaction front distribution could be observed inside the flames. Figure 11 shows these fluctuations recorded in the vicinity of the rearward facing step in time steps of 40 ms comparing a single hole injector and a twin hole injector. The initial air Mach number was $M_\infty = 0.2$ and the hydrogen was injected with an injection angle of $\alpha = 45°$ with a specific mass flow rate of $(\rho w)_{H_2} = 55.7$ kg m$^{-2}$ s$^{-1}$. It can be seen that using a twin hole injector, the fluctuations or oscillations are much greater compared with the single hole injector. This can be explained by the reduced impact of three-dimensional vortex structures on the mixing jet described earlier in this article (see Section 2.1). These vortices effect a homogenization of the local hydrogen/air mixing ratio inside the inner border of the mixing jet, where the flames are stabilized. This homogenization leads to a reduction of the flame oscillation by avoiding temporal fluctuations of the hydrogen/air mixing ratio. When looking at the images taken with the single hole injector, it can be seen that the flame oscillations are smaller compared with the twin hole injector. This is due to the great impact of three-dimensional vortex structures, as they are described in Section 2.1 of this article.

The experiments showed that, in general, an increase of the initial air Mach number led to a strong reduction of these flame oscillations, whereas an increasing specific mass flow rate for hydrogen enhanced the oscillations.

## 4. SUMMARY AND CONCLUDING REMARKS

The experimental investigation of sub- and supersonic hydrogen/air flames by means of optical measurement techniques showed that the mixing and combustion process was very much influenced by the type of injector used, the injection angle, the specific mass flow rate of fuel and the initial air Mach number. The growth and development of the mixing jet could be calculated by using the presented equations (2) and (5), which were in very good agreement with the experimental data. The application of a rearward facing step as a turbulence promotor enhanced the mixing process and contributed to avoid the blockage of the main air flow by compensating the additional mass flow rate of the injected fuel with an enlargement of the combustion chamber cross-section. Furthermore, the rearward facing step enabled the stabilization of the hydrogen/air flames inside the free shear layer separating the mixing jet and the recirculation zone generated in the wake of the rearward facing step. Without the use of the rearward facing step, the flames could only be stabilized up to initial air Mach numbers of $M_\infty = 0.1$, which can be explained by the presented model for flame stabilization. The results of the 'cold mixing experiments' were in very good agreement with the 'hot combustion experiments', so that the combustion processes could be predicted by using the data received from the mixing experiments.

The presented work, which was sponsored by the German Research Society (DFG), will be continued with respect to a detailed investigation of the temperature profile of the hydrogen/air flames. Thereby the influence of a multihole injection geometry in a cascade of rearward facing steps on the homogenization of the flame temperature profile with respect to $NO_x$ will be investigated.

## REFERENCES

1. M. Oschwald, R. Guerra and W. Waidmann, Investigation of the flow field of a scramjet combustor with parallel hydrogen injection through a strut by particle image displacement velocimetry, *Proceedings of the 3rd International Symposium on special topics in chemical propulsion*, pp. 113–115. The Pennsylvania State University, University Park, PA (1993).
2. R. J. Fuller, R. B. Mays, R. H. Thomas and J. A. Schetz, Mixing studies of helium and air at high supersonic speeds, *AIAA J.* **30**, 2234–2243 (1992).
3. R. J. Bakos, J. Tamagno, O. Rizkalla, M. V. Pulsonetti, W. Chinitz and J. I. Erdos, Hypersonic mixing and combustion studies in the hypulse facility, *J. Propulsion Power* **8**, 900–906 (1992).
4. M. P. Lee, B. K. McMillin, J. L. Palmer and R. K. Hanson, Planar fluorescence imaging of a transverse jet in a supersonic cross flow, *J. Propulsion Power* **8**, 729–735 (1992).
5. J. A. Schetz, F. S. Billig and S. Favin, Analysis of slot injection in hypersonic flow, *J. Propulsion Power* **7**, 115–122 (1991).
6. J. A. Schetz, R. H. Thomas and P. S. King, Combined tangential normal injection into supersonic flow, *J. Propulsion Power* **7**, 420–430 (1991).
7. E. J. Fuller, R. H. Thomas and J. A. Schetz, Effects of yaw on low angle injection into supersonic flow, AIAA paper 91-0014. American Institute of Aeronautics and Astronautics, Washington, D.C. (1991).
8. M. Takahashi and A. K. Hayashi, Numerical study on the mixing and combustion of injecting hydrogen jets in a supersonic air flow, AIAA Paper 91-0574. American Institute of Aeronautics and Astronautics, Washington, D.C. (1991).
9. T. R. A. Bussing and G. L. Lidstone, Transverse fuel injection model for a scramjet propulsion system, *J. Propulsion Power* **6**, 355–356 (1990).
10. N. L. Messerschmith, S. G. Goebel, J. P. Renie, J. C. Dutton and H. Krier, Investigation of a supersonic mixing layer, *J. Propulsion Power* **6**, 353–354 (1990).
11. J. A. Schetz, R. H. Thomas and F. S. Billig, Gaseous injection in high speed flow, *Proceedings of the Ninth International Symposium on Air Breathing Engines*, Vol. 1, pp. 1–16. American Institute of Aeronautics and Astronautics, Washington, D.C. (1989).
12. J. A. Schetz, R. H. Thomas and P. S. King, Combined tangential–normal injection into a supersonic flow, AIAA Paper 89-0622. American Institute of Aeronautics and Astronautics, Washington, D.C. (1989).
13. J. A. Schetz, S. Favin and F. S. Billig, Simplified analysis of slot injection in hypersonic flow, AIAA Paper 88-3056. American Institute of Aeronautics and Astronautics, Washington, D.C. (1988).
14. S. C. Lee, Turbulent mixing of coaxial jets between hydrogen and air, *Int. J. Hydrogen Energy* **11**, 807–816 (1986).
15. J. A. Schetz, *Injection and Mixing in Turbulent Flow*. American Institute of Aeronautics and Astronautics, New York (1980).
16. R. C. Rogers, A study of the mixing of hydrogen injected

normal to a supersonic airstream, NASA TN D-6114 (1971).
17. W. Hauf and U. Grigull, *Optical Methods in Heat Transfer*. Academic Press, New York (1970).
18. F. Mayinger, *Optical Measurement Techniques*. Springer, Berlin (1994).
19. F. Mayinger and W. Panknin, Holography in heat and mass transfer, *International Heat Transfer Conference*, Tokyo, Vol. 6, p. 27 (1978).
20. M. Haibel, F. Mayinger and G. Strube, Application of non-intrusive diagnostic methods to sub- and supersonic hydrogen/air flames, *Proceedings of the 3rd International Symposium on special topics in chemical propulsion*, pp. 109–112. The Pennsylvania State University, University Park, PA (1993).
21. A. G. Gaydon, *The Spectroscopy of Flames* (2nd Edn). Chapman and Hall, London (1974).
22. R. Guerra, W. Waidmann and C. Laible, An experimental investigation of the combustion of a hydrogen jet injected parallel in a supersonic air stream, AIAA Paper 91-5102. American Institute of Aeronautics and Astronautics, Washington, D.C. (1991).
23. R. C. Orth and J. A. Funk, An experimental and comparative study of jet penetration in supersonic flow, *J. Spacecraft Rockets* **4**, 1236–1242 (1967).
24. N. Brehm and F. Mayinger, Turbulent flame acceleration: the transition from deflagration to detonation, *Proceedings of the 2nd International Symposium on Heat Transfer*, Beijing, p. 581 (1988).
25. F. Mayinger and G. Strube, Hydrogen combustion: safety hazards in hydrogen systems, *Proceedings of the International Conference on the Analysis of Thermal and Energy Systems*, Athens, Vol. 2, pp. 1021–1032 (1991).
26. R. Beauvais and F. Mayinger, Influence of the flow structure on the propagation of hydrogen/air flames, BMFT-RS 1500 810, FIZ, Karlsruhe, FRG (1994).